

ORIGINAL ARTICLE

Open Access



# African swine fever virus MGF505-3R inhibits cGAS-STING-mediated IFN- $\beta$ pathway activation by degrading TBK1

Mingyang Cheng<sup>1,2,3,4</sup>, Jiawei Luo<sup>1</sup>, Yuetong Duan<sup>1</sup>, Yu Yang<sup>1</sup>, Chunwei Shi<sup>1,2,3,4</sup>, Yu Sun<sup>1,2,3,4</sup>, Yiyuan Lu<sup>1,2,3,4</sup>, Junhong Wang<sup>1,2,3,4</sup>, Xiaoxu Li<sup>1,2,3,4</sup>, Jianzhong Wang<sup>1,2,3,4</sup>, Nan Wang<sup>1,2,3,4</sup>, Wentao Yang<sup>1,2,3,4</sup>, Yanlong Jiang<sup>1,2,3,4</sup>, Guilian Yang<sup>1,2,3,4</sup>, Yan Zeng<sup>1,2,3,4\*</sup>, Chunfeng Wang<sup>1,2,3,4\*</sup> and Xin Cao<sup>1,2,3,4</sup>

## Abstract

African swine fever virus (ASFV) is an important pathogen causing acute infectious disease in domestic pigs and wild boars that seriously endangers the global swine industry. As ASFV is structurally complex and encodes a large number of functional proteins, no effective vaccine has been developed to date. Thus, dissecting the mechanisms of immune escape induced by ASFV proteins is crucial. A previous study showed that the ASFV-encoded protein is an important factor in host immunity. In this study, we identified a negative regulator, MGF505-3R, that significantly downregulated cGAS/STING- and poly (dG:dC)-mediated IFN- $\beta$  and interferon stimulation response element (ISRE) reporter activity and suppressed IFNB1 and IFIT2 mRNA levels. In addition, TBK1, IRF3 and I $\kappa$ B $\alpha$  phosphorylation levels were also inhibited. Mechanistically, MGF505-3R interacted with cGAS/TBK1/IRF3 and targeted TBK1 for degradation, thereby disrupting the cGAS-STING-mediated IFN- $\beta$  signaling pathway, which appears to be highly correlated with autophagy. Knockdown MGF505-3R expression enhanced IFN- $\beta$  and IL-1 $\beta$  production. Taken together, our study revealed a negative regulatory mechanism involving the MGF505-3R-cGAS-STING axis and provided insights into an evasion strategy employed by ASFV that involves autophagy and innate signaling pathways.

**Keywords:** African swine fever virus, MGF505-3R, cGAS/STING signaling pathway, TBK1, Innate immunity

## Introduction

African swine fever (ASF) is an acute, hemorrhagic, and highly contagious infectious disease caused by the African swine fever virus (ASFV) that has an acute mortality rate of up to 100%, and no effective vaccines or treatments have been developed (Dixon et al. 2020; Dixon et al. 2019b). The prevalence of ASFV not only greatly damages the global swine economy but also seriously endangers public health security (Sun et al. 2021b). ASFV

is a complex icosahedral DNA virus and is the only member of the *Asfarviridae* family (Wang et al. 2021). The virus consists of four layers of a concentric axial structure and a hexagonal outer membrane that is formed as the virus buds through the cell membrane (Liu et al. 2019). ASFV replication occurs mainly in the cytoplasm of infected macrophages, although early replication of the virus is also observed within the nucleus (Forth et al. 2020). ASFV genome is quite large, approximately 170–193 kb, and encodes 150–200 proteins (Portugal et al. 2020). Previous studies have shown that the key virulence gene family members MGF505-7R and 11R potently antagonize IFN-I production (Li et al. 2021a). However, further studies are

\* Correspondence: [zengyan@jlu.edu.cn](mailto:zengyan@jlu.edu.cn); [wangchunfeng@jlu.edu.cn](mailto:wangchunfeng@jlu.edu.cn); [xinc@jlu.edu.cn](mailto:xinc@jlu.edu.cn)

<sup>1</sup>College of Veterinary Medicine, Jilin Agricultural University, Changchun, China

Full list of author information is available at the end of the article



© The Author(s). 2022 **Open Access** This article is licensed under a Creative Commons Attribution 4.0 International License, which permits use, sharing, adaptation, distribution and reproduction in any medium or format, as long as you give appropriate credit to the original author(s) and the source, provide a link to the Creative Commons licence, and indicate if changes were made. The images or other third party material in this article are included in the article's Creative Commons licence, unless indicated otherwise in a credit line to the material. If material is not included in the article's Creative Commons licence and your intended use is not permitted by statutory regulation or exceeds the permitted use, you will need to obtain permission directly from the copyright holder. To view a copy of this licence, visit <http://creativecommons.org/licenses/by/4.0/>. The Creative Commons Public Domain Dedication waiver (<http://creativecommons.org/publicdomain/zero/1.0/>) applies to the data made available in this article, unless otherwise stated in a credit line to the data.

required to understand the immune escape mechanisms of ASFV.

Innate immunity is the first line of defense that is gradually formed during the ontogenetic evolution of the germline (Briard et al. 2020). Viral dsDNA is localized close to the plasma membrane following specific recognition by cyclic GMP-AMP synthase (cGAS) (Cai et al. 2022), which dimerizes to form a complex and binds to both double-stranded DNA strands (Ma et al. 2018). cGAS-dsDNA binding induces a conformational phase transition for the ATP- and GTP-catalyzed synthesis of cGAMP (Zhang et al. 2020b), which binds to stimulator of interferon genes (STING) and recruits TANK binding kinase 1 (TBK1) or I-kappaB kinase epsilon (IKKe). These kinases activate interferon regulatory factor 3 (IRF3) or inhibitor kappa B alpha (IkBa) to produce type I interferon and proinflammatory cytokines (Yang et al. 2022b).

Interferons (IFNs) are cytokines produced by cells in response to exogenous antigens and are classified into three types, including type I interferon (IFN-I), type II interferon (IFN-II) and type III interferon (IFN-III), depending on the interferon receptor. Although these IFNs all share the common property of limiting viral replication, IFN- $\beta$  is generally considered the most widespread antiviral factor among IFN-I members (Ivashkiv and Donlin 2014). IFN- $\beta$  forms an ISGF3 trimer by binding to the interferon receptor and then recruiting the associated kinase, which subsequently enters the nucleus to bind the interferon-stimulated gene (ISG) promoter and initiate the transcription of antiviral-related genes. Among the many ISGs, ISG15 is considered to be the most strongly expressed and fastest ubiquitin-like protein during viral infections (Yan et al. 2021). IFIT family proteins are also widely involved in antiviral immunity. In previous studies, IFIT1 (ISG56) and IFIT2 (ISG54) were shown to protect against a variety of viral infections, including sendai virus (SeV) and vesicular stomatitis virus (VSV) (Fensterl et al. 2014; Wetzel et al. 2014). Ubiquitination modifications also play a critical function in the IFN signaling cascade, and TBK1 is regulated by multiple E3 ubiquitin ligases and deubiquitination as the hub of the cGAS-STING-mediated IFN- $\beta$  signaling axis. Ring finger protein 128 (RNF-128) inhibits viral replication by interacting with TBK1 to catalyze K63-linked polyubiquitination of TBK1 (Song et al. 2016). RNF138 is a less studied E3 ubiquitination ligase, and Huang et al. found that the ASFV HLJ/18 strain protein inhibited the conversion of RNF138 to RNF128 (Huang et al. 2021).

Autophagy is a type of programmed cell death mediated mainly by lysosomes where cells undergo fusion with lysosomes after receiving autophagy-inducing signals that regulate autophagy-related genes (ATGs)

followed by detached membranes that wrap around the cytoplasm to form bilayer membrane structures of autophagic precursors (Choy and Roy 2013). Autophagy-lysosomes initiate a clearance program for proteins or damaged organelles. Furthermore, upon cGAMP binding, STING interacts with LC3 and promotes noncanonical autophagy through an ATG5-dependent mechanism following TBK1 degradation to control viral replication (Zahid et al. 2020).

ASFV has long evolved multiple strategies to escape innate immunity through competition with the host, the most widely reported of which is the inhibition of IFN-I signaling axis action (Dixon et al. 2019a). The recombinant virus ASFV-G- $\Delta$ MGF with six MGF360/MGF505 genes deleted (MGF360-12/13/14L; MGF505-1/2/3R) was shown to be fully attenuated *in vivo*, indicating that the MGF360 and MGF505 families are key virulence genes for ASFV (O'donnell et al. 2015). Recent studies have shown that MGF505-7R degrades STING by promoting the autophagy-related protein ULK1 (Li et al. 2021a) and promotes the degradation of JAK1 and JAK2 by upregulating the expression of the E3 ubiquitin ligase RNF125 (Li et al. 2021b). In addition to the well-known IFN-I suppressor genes, other ASFV gene-encoded proteins have also been gradually discovered for their function in escaping innate immunity. For example, ASFV- $\Delta$ pE66L recombinant virus induces higher levels of IFNB1 and TNF- $\alpha$  expression than its parental counterpart (Shen et al. 2020). In addition, pI215L binds RNF138 and inhibits type I IFN production and K63-linked polyubiquitination of TBK1 (Huang et al. 2021), and DP96R weakens TBK1 phosphorylation to impair antiviral immunity (Wang et al. 2018).

In the present study, we demonstrate that ASFV MGF505-3R is a negative regulator of the cGAS-STING DNA sensing pathway that controls IFN- $\beta$  production. Mechanistically, ASFV MGF505-3R interacted with cGAS/TBK1/IRF3 and impaired TBK1 expression by autophagy. Our findings reveal a protein that facilitates ASFV escape from innate immunity and provide new theoretical support for the development of attenuated ASFV vaccines in the future.

## Results

### MGF505-3R inhibits cGAS-STING-mediated signaling

To verify whether ASFV MGF505-3R specifically inhibits the cGAS-STING-mediated IFN-I signaling pathway, HEK293T cells were cotransduced with reporter gene plasmids and the indicated expression plasmids. The results revealed that ASFV MGF505-3R inhibited cGAS-STING-mediated IFN- $\beta$  (Fig. 1A) and ISRE reporter activity (Fig. 1B) but not MyD88-mediated NF- $\kappa$ B reporter activity (Fig. 1C). Poly (dG:dC) (dsDNA) is a cytosolic DNA sensor (CDS) agonist that specifically

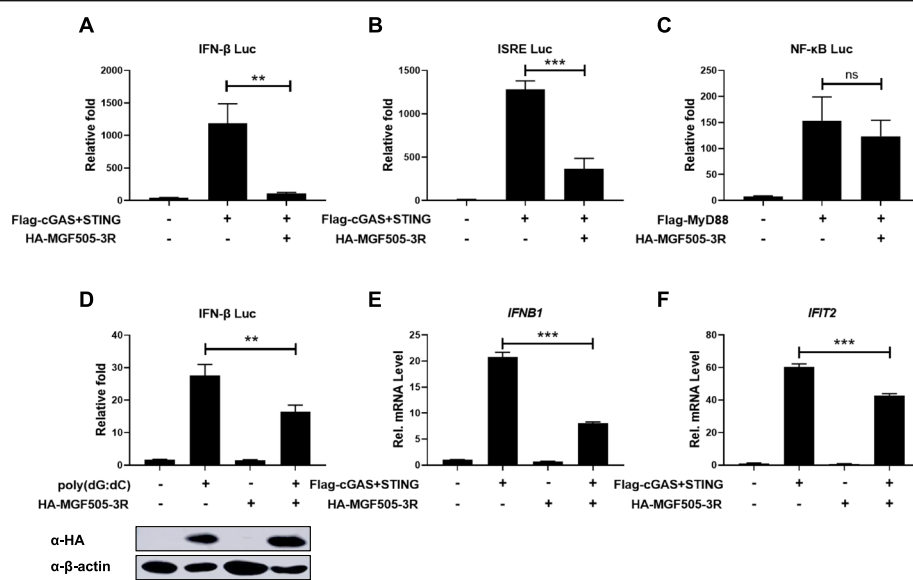


**Fig. 1** MGF505-3R inhibited the cGAS-STING-mediated IFN- $\beta$  signaling pathway. **A-C** HEK293T cells were cotransfected with IFN- $\beta$  promoter, ISRE, or NF-κB luciferase reporter plasmids (100 ng); pRL-TK plasmid (50 ng) and the indicated plasmids (200 ng) (pCMV-N-HA was chosen as a negative control). Twenty-four hours after transfection, HEK293T cells were used for dual-luciferase reporter assays. **D** Twenty hours after transfection of HA-MGF505-3R, the cells were left untreated or treated with poly (dG:dC) (500 ng) for 12 h before use in dual-luciferase reporter assays. MGF505-3R expression was analyzed by western blotting using an anti-HA antibody. **E-F** HEK293T cells were transfected with the Flag-cGAS/Flag-STING expression plasmids (500 ng) and HA-MGF505-3R expression plasmid (1  $\mu$ g). Twenty-four hours after transfection, the cells were used for qRT-PCR analysis. "+" represents transfected, "-" represents nontransfected. All experiments were repeated independently at least thrice. The data from independent experiments are presented as the mean  $\pm$  SD;  $n=3$ . \* $P<0.05$ , \*\* $P<0.01$ , \*\*\* $P<0.001$ .

induces the cGAS-STING signaling axis to trigger the IFN-I signaling cascade (Yoneda et al. 2016). Therefore, we utilized poly (dG:dC) to mimic the viral DNA. Similar conclusions were obtained that poly (dG:dC) stimulation with MGF505-3R inhibited IFN- $\beta$  signaling activated by the DNA analog (Fig. 1D). In addition, MGF505-3R significantly downregulated the transcript levels of IFNB1 (Fig. 1E) and IFIT2 (Fig. 1F) due to cGAS/STING overexpression, as shown by qRT-PCR ( $P<0.001$ ).

**MGF505-3R hinders TBK1, IRF3 and I $\kappa$ B $\alpha$  phosphorylation**  
IRF3 and I $\kappa$ B $\alpha$ , molecules downstream of TBK1 and IKK $\epsilon$ , are key transcription factors for IFN- $\beta$  during cGAS-STING-mediated signaling. TBK1 undergoes autoprophosphorylation to phosphorylate cytoplasmic IRF3, which then translocates to the nucleus to activate transcription that leads to IFN-I production. To further determine the immunosuppressive function of MGF505-3R, phosphorylation levels of TBK1, I $\kappa$ B $\alpha$  and IRF3 were assessed by immunoblotting. The results showed that ASFV MGF505-3R downregulated cGAS/STING overexpression-stimulated I $\kappa$ B $\alpha$  phosphorylation (Fig. 2A, B). In a subsequent experiment, we found that MGF505-3R overexpression with poly (dG:dC) to mimicking viral infection similarly decreased TBK1 (Fig. 2C, D), IRF3 (Fig. 2C, E), and I $\kappa$ B $\alpha$  phosphorylation levels

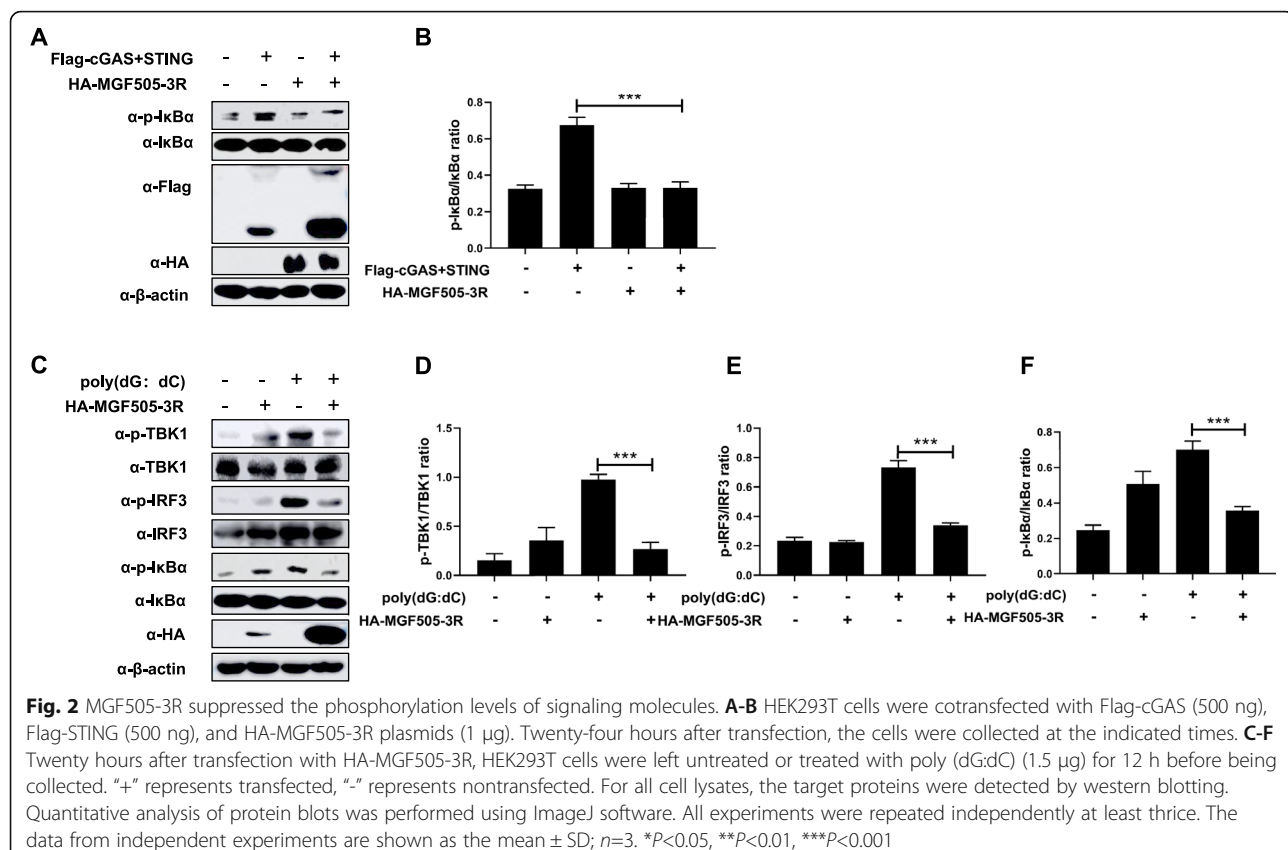
(Fig. 2C, F). Collectively, ASFV MGF505-3R inhibited IFN- $\beta$  production by controlling the cGAS-STING signaling pathway.

#### MGF505-3R inhibits the activation of IFN- $\beta$ promoters through STING, TBK1, and IRF3

To search for the immunosuppressive site targeted by ASFV MGF505-3R, HEK293T cells were cotransformed with the MGF505-3R plasmid and signaling molecule plasmids followed by analysis of the restriction of IFN- $\beta$  activity by MGF505-3R using a dual-luciferase reporter gene. The results revealed that ASFV MGF505-3R not only inhibited IFN- $\beta$  activation but also suppressed cGAS/STING expression in a dose-dependent manner, which further explained the results of Fig. 1A (Fig. 3A). However, IFN- $\beta$  signaling activated by STING (Fig. 3B), TBK1 (Fig. 3C), and IRF3 (Fig. 3E) but not IKK $\epsilon$  (Fig. 3D) alone was also effectively controlled by MGF505-3R. Interestingly, MGF505-3R inhibited IFN- $\beta$  activity mediated by IRF3; however, it did not restrict IRF3 protein expression. This finding may potentially imply that MGF505-3R can control the IFN- $\beta$  signaling cascade further downstream.

#### MGF505-3R interacts with cGAS, TBK1 and IRF3

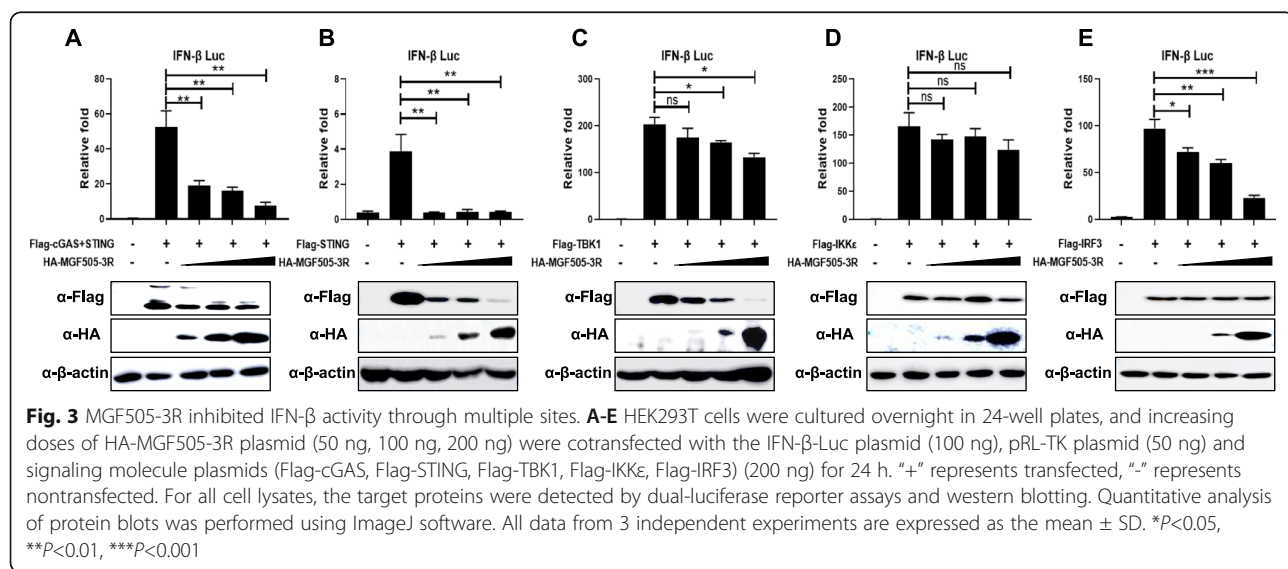
To elucidate the mechanism of the role of ASFV in the innate immune response, the interactions between

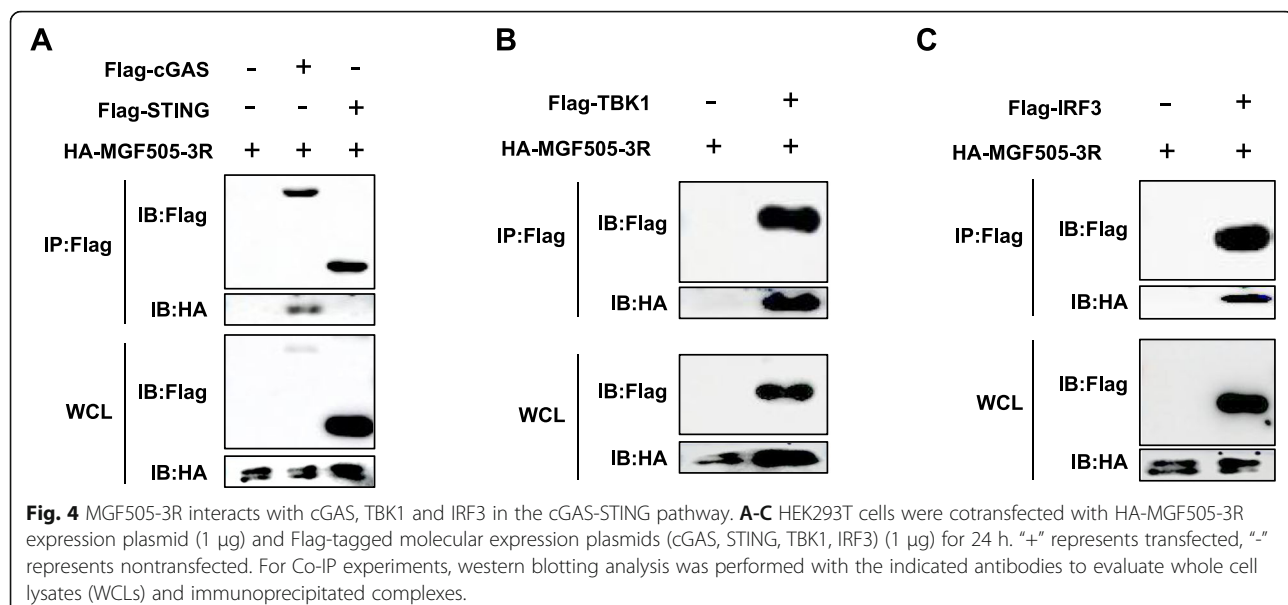


MGF505-3R and signal transduction molecules were examined by coimmunoprecipitation (Co-IP). cGAS, STING, TBK1 and IRF3 plasmids were cotransfected with the MGF505-3R plasmid in HEK293T cells. Co-IP experiment results revealed that cGAS (Fig. 4A), TBK1 (Fig. 4B), and IRF3 (Fig. 4C) interact with ASFV MGF505-3R.

#### MGF505-3R mediates autophagic degradation of TBK1

The above studies have demonstrated that the weakening of the antiviral response is closely related to the interaction between MGF505-3R and cGAS, TBK1, and IRF3, and we wanted to assess whether interference with signal molecule expression occurred. The results indicated that MGF505-3R degraded the cGAS (Fig. 5A),





STING (Fig. 5B) and TBK1 (Fig. 5C), especially, higher doses of MGF505-3R provided stronger inhibition on STING and TBK1. cGAS was transiently repressed and subsequently activated, whereas IKKe (Fig. 5D) and IRF3 (Fig. 5E) expression was not affected. To date, we have confirmed that MGF505-3R impairs TBK1 expression and phosphorylation. In parallel, MGF505-3R dose-dependently inhibited IFN- $\beta$  activity mediated by TBK1. In fact, this action could be potentially linked to the interaction between MGF505-3R and TBK1. Given that a preponderance of the data pointed to TBK1, we hypothesized that it is a key target of MGF505-3R and therefore further investigated the mechanism of TBK1 degradation. 3-Methyladenine (3-MA) is an inhibitor of PI3K that specifically blocks the formation of autophagosomes and is widely used as an inhibitor of cellular autophagy. Interestingly, MGF505-3R-mediated TBK1 degradation was reversed upon the addition of 3-MA (Fig. 5F, G). Accordingly, MGF505-3R might be involved in autophagy pathways to degrade TBK1.

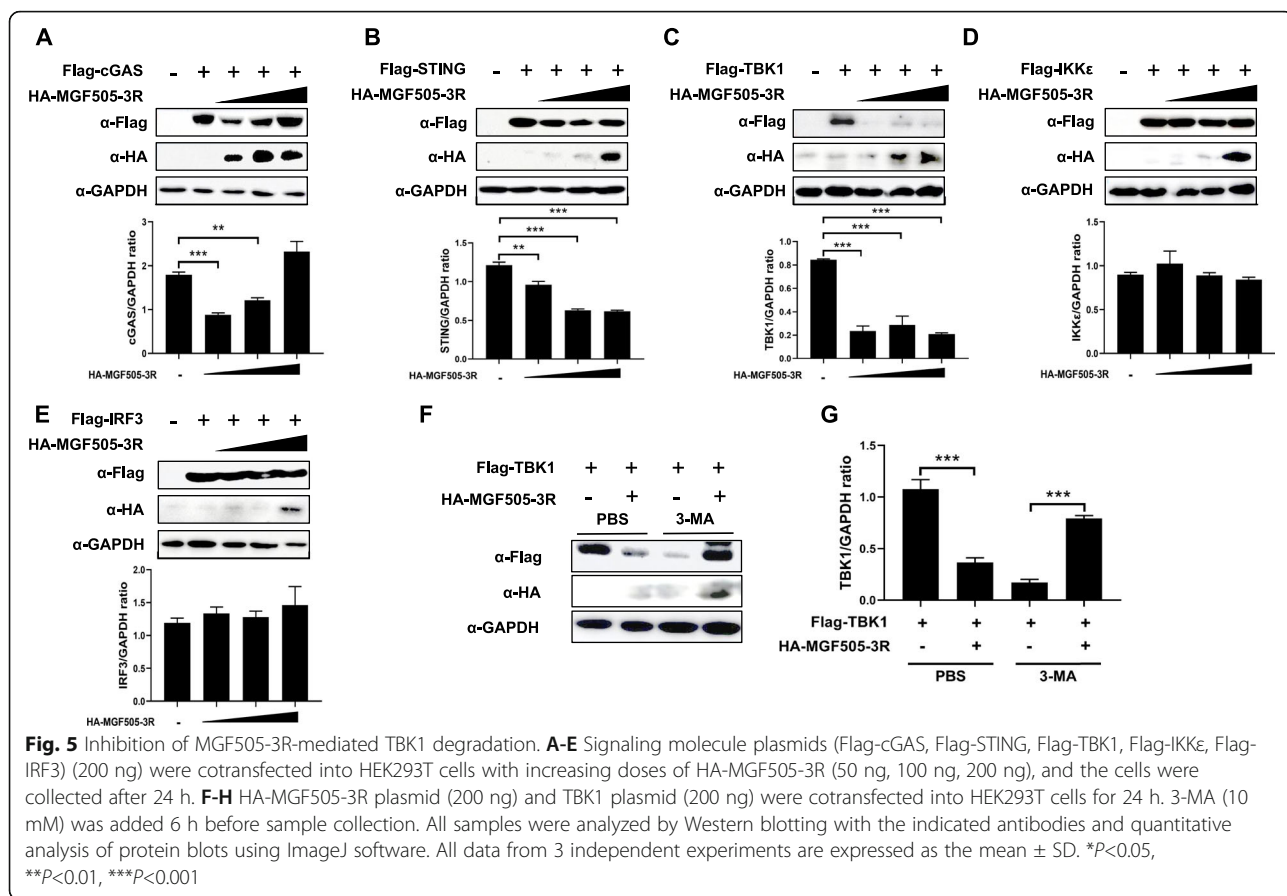
#### MGF505-3R knockdown promotes antiviral levels in PAMs infected with AFSV

To further validate the antagonistic effect of MGF505-3R on antiviral immunity, we synthesized a specific siRNA against MGF505-3R to achieve knockdown of protein expression. Consistent with our previous study on HEK293T cells (Fig. 1E, F), knockdown of MGF505-3R expression enhanced the gene transcription levels of ISGs in PAMs after AFSV infection (Fig. 6A-D). In addition, significant upregulation of IL-1 $\beta$  levels in cell culture supernatants at 24 h ( $P<0.01$ ) but not 12 h was involved in counteracting viral infection (Fig. 6E). Further analysis revealed that siMGF505-3R upregulated

IRF3 phosphorylation levels compared with the nontargeted control siRNA. p54 is an important structural protein of AFSV that is involved in viral particle assembly and viral adhesion to host cells. We also found that the knockdown of MGF505-3R resulted in the diminished expression of p54 protein (Fig. 6F-H).

#### Discussion

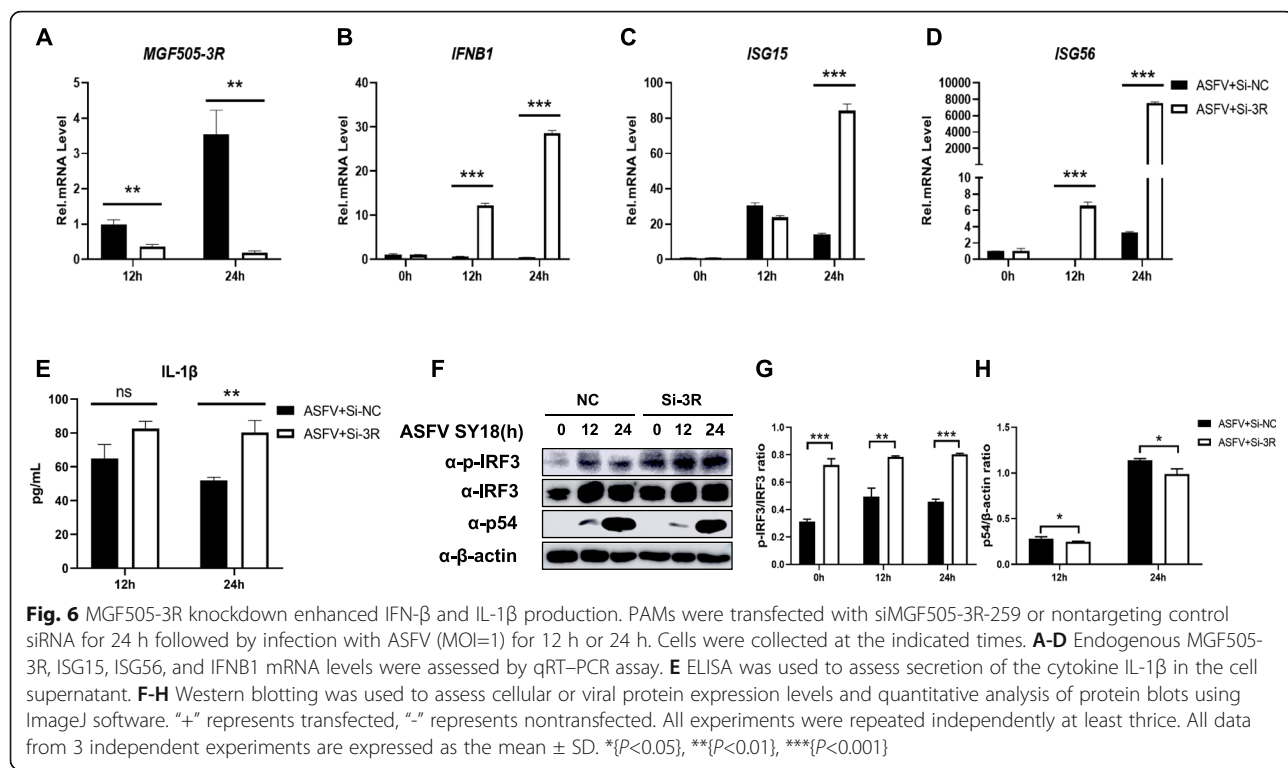
The innate immune system is essential for the detection of viruses and constitutes the first line of defense. Viral components are sensed by host pattern recognition receptors (PRRs) (Webb and Fernandez-Sesma 2022). cGAS, a key receptor for dsDNA, initiates immune responses against most DNA viruses through the STING-TBK1 signaling pathway (Zhang et al. 2020a). However, viruses will achieve competitive evolution with their hosts through newer immune escape strategies (Cuesta-Geijo et al. 2022). Previous studies have shown that the virulent AFSV Armenian/07 strain suppresses the IFN- $\beta$  signaling pathway by impairing STING (García-Belmonte et al. 2019). A large amount of work was subsequently directed at the encoded proteins of the virus. STAT1 and STAT2 are important downstream signals of IFN-I that can be targeted for degradation by MGF360-9L (Zhang et al. 2022). MGF505-11R has also been found to be effective in limiting IFN- $\beta$  production (Yang et al. 2021b). In this study, we used reporter gene screening for proteins encoded by the MGF505 family (results not shown) and found that MGF505-3R, a negative regulator of virulence, was able to inhibit cGAS-STING-mediated IFN- $\beta$  and ISRE reporter gene activity but not MyD88-mediated NF- $\kappa$ B signaling, indicating that it is required for targeting cGAS-STING.



Activation of TBK1, IRF3 and I $\kappa$ B $\alpha$  is critical for initiating antiviral immune responses. TBK1 is an important molecule that bridges IFN-I signaling and upon activation phosphorylates and nucleates the downstream transcription factor IRF3. I $\kappa$ B $\alpha$  is an important signal for NF- $\kappa$ B production, and activation of IKK $\epsilon$  triggers I $\kappa$ B $\alpha$  phosphorylation, which is also essential to enhance IFN- $\beta$  and inflammatory factor production. However, these molecules are controlled by the host to maintain immune homeostasis. Neural precursor cell expressed developmentally downregulated protein 4 (NEDD4), for example, has been shown to be a switch that mediates TBK1 to maintain innate immune homeostasis (Gao et al. 2021). Critically, TBK1 is subject to extensive regulation. Specifically, K63-linked ubiquitination of TBK1 mostly occurs in the early stages of viral infection, whereas K48-linked ubiquitination occurs in the late stages. In addition to ubiquitination, it has been shown that the methyltransferase PRMT1 similarly increases TBK1 methylation modifications, increasing autoprophosphorylation (Wu et al. 2021). IRF3 was also found to be regulated by a number of proteins, including EF-hand protein calmodulin-like 6 (CALML6) and the mitochondrial protein ERAL1 (Li et al. 2021d; Wang et al. 2019). These normal immune signals will often become targets

of viral attack, disrupting immune homeostasis and thereby interfering with IFN- $\beta$  production. These pathways will also form the basis for studying the antagonism of innate immunity by ASFV. Reports have suggested that TNF- $\alpha$ -activated p-I $\kappa$ B $\alpha$  is significantly inhibited by the ASFV CN/GS/2018 strain F317L (Yang et al. 2021a), and IRF3 phosphorylation was markedly decreased in PK-15 or HEK293T cells in the presence of E120R after poly (dA:dT) stimulation (Liu et al. 2021). Our data showed that MGF505-3R suppressed TBK1, IRF3, and I $\kappa$ B $\alpha$  phosphorylation levels and interacts with TBK1 for subsequent degradation, thereby inhibiting IFN- $\beta$  signaling.

Protein degradation is one of the main strategies to regulate protein function in biological processes, and cellular autophagy is a crucial program. However, viruses can aid their replication by manipulating autophagy. For example, the 2AB protein of Senecavirus A antagonizes selective autophagy by degrading LC3 (Sun et al. 2021a), and the FMDV capsid protein VP2 induces autophagic escape immunity by interacting with HSPB1 (Sun et al. 2018). The mechanisms by which RNA viruses regulate host autophagy are well understood, but reports on ASFV are limited. In 2013, Hernaez et al. found that the ASFV A179L protein may inhibit host autophagy by



binding to Beclin-1 (Hernaez et al. 2013), representing an early report on this mechanism (Banjara et al. 2019). However, Shimmon et al. confirmed that A179L does not block the formation of autophagosomes (Shimmon et al. 2021). Subsequently, Li et al. found for the first time that ASFV MGF505-7R is involved in the cGAS-STING-mediated autophagic pathway (Li et al. 2021b). Recent studies also confirmed that several ASFV proteins, including pI215L and A137R, function to regulate autophagy-mediated lysosomal degradation of TBK1 (Sun et al. 2022). This finding indicates that escape of the natural immune response by ASFV-encoded proteins through control of the autophagic program is likely to be a fundamental strategy. Our results showed that TBK1 degradation by MGF505-3R was reversed after the addition of 3-MA, demonstrating that MGF505-3R may degrade TBK1 through autophagy. The autophagic process by which MGF505-3R degrades TBK1 will be further explored.

The ASFV multigene family MGF360 and MGF50 genes promote the survival of infected cells, allow the virus to replicate efficiently in macrophages and are closely related to the virulence of the virus. Knockdown of ASFV MGF505-11R/MGF360-11L expression using siRNA in PAMs resulted in reduced viral proliferation (Yang et al. 2022a). Similarly, MGF505-7R-deficient ASFV( $\Delta$ 7R) had a diminished replicative capacity and increased antiviral levels *in vivo* following infection of pigs (Li et al. 2021c). In a recent study in which we

attempted to knockdown MGF505-3R expression to further investigate the role of ASFV in porcine alveolar macrophages, knockdown of ASFV MGF505-3R using siRNA was shown to inhibit the expression of the early viral protein p54 (Fig. 6F, H) with significant upregulation of host antiviral capacity, including IFNB1/ISG15/ISG56 gene transcript levels, IRF3 phosphorylation and IL-1 $\beta$  production (Fig. 6A-F).

## Conclusions

In summary, our results demonstrate for the first time that ASFV MGF505-3R is involved in the innate immune response mediated by cGAS-STING. MGF505-3R potently inhibits IFN- $\beta$  by blocking p-TBK1, p-IRF3, and p-I $\kappa$ B $\alpha$ . Importantly, MGF505-3R interacts with TBK1 and most likely degrades it via the autophagy pathway. Furthermore, knockdown of MGF505-3R increases the expression of ISGs and secretion of IL-1 $\beta$ . This study identifies ASFV MGF505-3R as an inhibitor of the cGAS-STING pathway that plays an important role in blocking the production of IFN- $\beta$  and proinflammatory cytokines, suggesting the possibility of developing an attenuated ASFV vaccine with MGF505-3R deficiency (Fig. 7).

## Materials and methods

### Cells and viruses

Human embryonic kidney 293T cells (HEK293T) were purchased from ATCC and grown in Dulbecco's

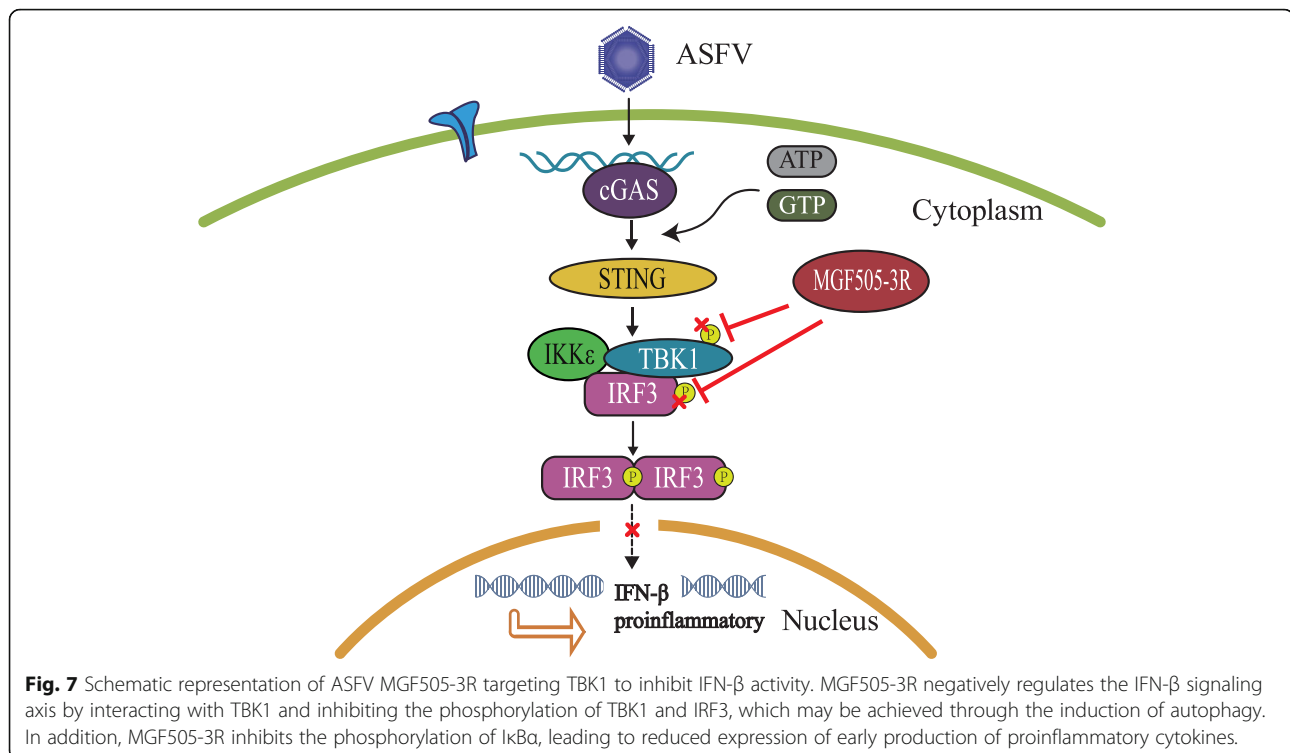


**Fig. 7** Schematic representation of ASFV MGF505-3R targeting TBK1 to inhibit IFN- $\beta$  activity. MGF505-3R negatively regulates the IFN- $\beta$  signaling axis by interacting with TBK1 and inhibiting the phosphorylation of TBK1 and IRF3, which may be achieved through the induction of autophagy. In addition, MGF505-3R inhibits the phosphorylation of I $\kappa$ B $\alpha$ , leading to reduced expression of early production of proinflammatory cytokines.

modified Eagle's medium (DMEM) supplemented with 10% fetal bovine serum (FBS) (Gibco), 100 U/ml penicillin, and 100  $\mu$ g/ml streptomycin. The isolation and culture of porcine alveolar macrophages (PAMs) was based on the procedure of Yang et al. (Yang et al. 2021b). The lungs of 4-week-old specific pathogen-free (SPF) piglets were flushed thrice using PBS with 2% penicillin-streptomycin, and the lavage fluid was centrifuged and resuspended for counting in RPMI-1640 (10% FBS, 1% penicillin-streptomycin, 2 mM L-glutamine). All cells were cultured and maintained at 37 °C with 5% CO<sub>2</sub>.

#### Virus experiments

The ASFV SY18 strain (GenBank: MH766894) was isolated from infected pigs and quantified by a 50% hemadsorptive dose (HAD50) assay. Briefly, porcine alveolar macrophages were seeded into 96-well plates. Then, blood or virus was diluted, and cells were infected. The rosette-like structure was observed continuously for 7 d, and viral hemadsorption units were calculated. ASFV cultivation and cell experiments were conducted in an animal biosafety level 3 lab (ABSL-3).

#### Construction and transfection of plasmids

Gene synthesis was performed according to the sequence of MGF505-3R in ASFV SY18 (GenBank: MH766894) using standard biology techniques, and the fragment was inserted into a pCMV-N-HA eukaryotic expression vector with EcoRI and NotI

digestion sites to generate HA-tagged expression plasmids. Plasmids for Flag-tagged cGAS, STING, TBK1, IKK $\epsilon$ , and IRF3; luciferase reporter plasmids IFN- $\beta$ -Luc, ISRE-Luc and NF- $\kappa$ B-Luc; and pRL-TK were described in previous studies (Wang et al. 2018). All constructed plasmids were confirmed by DNA sequencing. The recombinant plasmid DNA was extracted using the Plasmid Preparation Purification Kit (Omega), and the purified plasmids were transfected into HEK293T cells after incubation for 15 min in a 1:2 ratio of DNA to Lipofectamine™3000 transfection reagent Kit (Thermo Fisher).

#### Antibodies and reagents

Anti-GAPDH antibodies, anti- $\beta$ -actin antibodies, anti-Flag agarose affinity gels, and mouse anti-Flag horseradish peroxidase (HRP) were purchased from Sigma. Anti-HA-HRP antibodies were purchased from Roche. The phospho-TBK1 (Ser172) antibody, phospho-IRF3 (Ser396) antibody, phospho-I $\kappa$ B $\alpha$  (Ser32) antibody, rabbit anti-IRF3 antibody, rabbit anti-TBK1 antibody, and rabbit anti-I $\kappa$ B $\alpha$  antibody were obtained from Cell Signaling Technology. Poly (dG:dC) (t1rl-pgcn) was purchased from InvivoGen; 3-methyladenine, DMSO, and NH<sub>4</sub>Cl were purchased from Sigma. A double-luciferase reporter assay kit was purchased from Promega. Lipofectamine™ 3000 was purchased from Thermo Fisher, and jetPRIME® was purchased from Polyplus.

### qRT-PCR Assay

Total RNA from HEK293T cells or PAMs transfected with the indicated molecules stimulated with or without poly (dG:dC) or ASFV was extracted using TRIzol (Takara), and 1 µg of total RNA was reverse transcribed by Moloney mouse leukemia virus (M-MLV) reverse transcriptase (Promega) according to the manufacturer's instructions. cDNA was subject to short-term storage at -20 °C. SYBR Green fluorescent dye (Takara) was added to the cDNA, and the mixture was assessed in a PCR system (Applied Biosystems 7500). All specific primers are shown in Table 1. The  $2^{-\Delta\Delta CT}$  method was used to analyze the relative mRNA expression levels of each gene, and GAPDH served as the internal reference gene for the samples. The qRT-PCRs were repeated with three biological and three technical replications.

### Dual-luciferase reporter assays

HEK293T cells were cultured overnight in 24-well plates and subsequently cotransfected with luciferase reporter plasmids, including IFN- $\beta$ -Luc, ISRE-Luc, NF- $\kappa$ B-Luc (100 ng), and pRL-TK plasmid (50 ng), and the indicated dose of MGF505-3R (50 ng, 100 ng, 200 ng) for 24 h. Cells were either left untreated or treated with poly (dG:dC) for 12 h. Poly (dG:dC) was transfected with Lipofectamine™3000 at 500 ng or 1.5 µg per well. Then, samples were collected at the indicated times. Cells were lysed on ice for 10 min using lysis solution according to the manufacturer's instructions, and the cell lysates were used for assaying firefly and Renilla activity. Firefly and Renilla luciferase activity was measured using a dual-luciferase reporter assay system (Promega), and the data were normalized to the transfection efficiency by dividing the firefly luciferase activity by the Renilla luciferase

activity. All reporter gene assays were repeated at least thrice.

### Western blotting

HEK293T cells were cultured overnight in 6- or 24-well plates followed by cotransfection of the indicated plasmids into the cells for 24 h. Samples were collected at the indicated times. Cells were lysed with RIPA buffer, and total cellular proteins were added proportionally to 5× SDS buffer and boiled for 10 min. Proteins were separated by electrophoresis on 10% SDS-polyacrylamide gels and then transferred to NC membranes (Merck Millipore). The membranes were blocked with 5% skim milk for 1 h at room temperature and incubated with the indicated antibodies overnight at 4 °C. After washing with TBST (1% Tween 20), the membranes were incubated with secondary antibodies for 1 h at room temperature. After washing with TBST, the protein bands were observed and imaged with an Amey Imager 600RGB. Quantification of the protein signal was performed using ImageJ software.

### Coimmunoprecipitation (Co-IP)

The indicated molecules plasmids were cotransfected with HEK-293T cells for 24 h. Cells were collected, and total proteins were released in NP-40 lysate containing 20 mM Tris-HCl, 150 mM NaCl, 1% NP-40, and 1 mM EDTA with protease inhibitor cocktail. Each sample was added to 1 ml of NP-40 lysate along with 30 µl of anti-Flag agarose affinity gel and incubated overnight at 4 °C. After three washes of agarose beads with 1 ml of NP-40 buffer, the immunoprecipitated complexes were subjected to Western blotting analysis.

### siMGF505-3R-mediated knockdown

Referring to the published ASFV MGF505-3R mRNA sequence in GenBank, we selected 255-, 259- and 281-bp sequences with the help of online small interfering RNA (siRNA) primer design software (<http://jura.wi.mit.edu/bioc/siRNA/home.php>) and designed and submitted three pairs of siRNAs for synthesis. Specific primer sequences (MGF505-3R-255, MGF505-3R-259, MGF505-3R-281) and one pair of negative control siRNA primer sequences (MGF505-3R-NC) were designed. The siRNA corresponding to the MGF505-3R target sequence or a nontargeting control was purchased from Sigma-Aldrich. The siRNAs are listed in Table 2. PAMs were cultured overnight in 6-well plates, and MGF505-3R-259-siRNA or NC-siRNA (1.5 µg) was transfected with jetPRIME® for 24 h. The cells were uninfected or infected with ASFV for 12 h or 24 h at a multiplicity of infection (MOI) of 1. Samples were collected at the indicated times. IFN- $\beta$  production in the cells was assessed by q-PCR and western blotting. IL-1 $\beta$  secretion

**Table 1** The primer sequences for qRT-PCR

Primers	Sequence (5'→3')
Hu IFN- $\beta$ 1-Forward	CAGCAATTTCAGTGTCAAGCT
Hu IFN- $\beta$ 1-Reverse	TCATCCTGCTTGAGGCAGTAT
Hu IFIT2-Forward	AAGCACCTAAAGGGCAAAAC
Hu IFIT2-Reverse	TGGGCCATGTGATAGTAGAC
Hu GAPDH-Forward	AAAATCAAGTGGGGCGATGCT
Hu GAPDH-Reverse	GGGCAGAGATGATGACCCTTT
Sus IFN- $\beta$ -Forward	GCTAACAGTGCATCCTCCAAA
Sus IFN- $\beta$ -Reverse	AGCACATCATAGCTATGGAAAGA
Sus ISG15-Forward	GATCGGTGCGCTGCCTTC
Sus ISG15-Reverse	CGTTGCTGCGACCCTTGT
Sus ISG56-Forward	AAATGAATGAAGCCCTGGAGTATT
Sus ISG56-Reverse	AGGGATCAAGTCCCACAGATTT
MGF505-3R-Forward	ACTGTTAGGACTGCACTGGC
MGF505-3R-Reverse	TGCCAGTTGAACAGCATCT

**Table 2** SiRNA sequences used in this study

Primers	Sequence (5'→3')
SiMGF505-3R-255-Forward	CGCCGUCGUAGGAGCCCCUAdTdT
SiMGF505-3R-255-Reverse	UAGGGCUCCUACGACGGCGdTdT
SiMGF505-3R-259-Forward	GUCGUAGGAGCCCCUAGAAAdTdT
SiMGF505-3R-259-Reverse	UUUCUAGGGCUCCUACGACdTdT
SiMGF505-3R-281-Forward	AAUACUAUGACCUGGUUAdTdT
SiMGF505-3R-281-Reverse	UAAACCAGGUCAUAGUAUUdTdT
SiNC-Forward	UUCUCCGAACGUGUCACGUTT
SiNC-Reverse	ACGUGACACGUUCGGAGAATT

into cell supernatants was assessed by ELISA (MEIM IAN).

### Statistical analysis

Data are expressed as the mean ± SD. Student's t test or one-way ANOVA was used for all statistical analyses, with at least three independent trials. All statistical analyses were performed using GraphPad Prism 8 software. \*P<0.05, \*\*P<0.01, and \*\*\*P<0.001 were defined as statistically significant.

### Supplementary Information

The online version contains supplementary material available at <https://doi.org/10.1186/s44149-022-00046-8>.

#### Additional file 1.

### Acknowledgments

We sincerely thank the Changchun Veterinary Research Institute, Chinese Academy of Agricultural Sciences for kindly providing the animal biosafety level 3 lab (ABSL-3).

### Authors' contributions

All authors have read and approved the final version of the manuscript. All authors have read and approved the final version of the manuscript. Designed the experiments: CMY, ZY and CX. Performed the experiments: CMY, SY, YY and LJW. Analyzed the data: CMY, SCW, WJH, LXX and DYT. Provided reagents and material: LYY, WJZ, WN, YWT, JYL and YGL. Wrote the paper: CMY, ZY, WCF and CX. Proofed the manuscript: CX.

### Funding

This work was supported by the National Natural Science Foundation of China (31941018, 32072888, U21A20261), China Agriculture Research System of MOF and MARA (CARS-35), Science and Technology Development Program of Jilin Province (YDZJ202102CXJD029, 20190301042NY, 20200402041NC) and Science and Technology Development Program of Changchun City (21ZY42).

### Availability of data and materials

Data will be shared upon request by the readers.

### Declarations

#### Ethics approval and consent to participate

Not applicable.

#### Consent for publication

Not applicable.

### Competing interests

The authors declare no competing interests.

### Author details

<sup>1</sup>College of Veterinary Medicine, Jilin Agricultural University, Changchun, China. <sup>2</sup>Jilin Provincial Key Laboratory of Animal Microecology and Healthy Breeding, Jilin Agricultural University, Changchun, China. <sup>3</sup>Jilin Provincial Engineering Research Center of Animal Probiotics, Jilin Agricultural University, Changchun, China. <sup>4</sup>Key Laboratory of Animal Production and Product Quality Safety of Ministry of Education, Jilin Agricultural University, Changchun, China.

Received: 30 March 2022 Accepted: 15 May 2022

Published online: 20 June 2022

### References

- Banjara, S., G. Shimmon, L. Dixon, C. Netherton, M. Hinds, and M. Kvansakul. 2019. Crystal Structure of African Swine Fever Virus A179L with the Autophagy Regulator Beclin. *Viruses* 11 (9): 789. <https://doi.org/10.3390/v11090789>.
- Briard, B., D. Place, and T. Kanneganti. 2020. DNA Sensing in the Innate Immune Response. *Physiology (Bethesda, Md.)* 35 (2): 112–124. <https://doi.org/10.1152/physiol.00022.2019>.
- Cai, H., C. Meignin, and J. Imler. 2022. cGAS-like receptor-mediated immunity: the insect perspective. *Current opinion in immunology* 74: 183–189. <https://doi.org/10.1016/j.coi.2022.01.005>.
- Choy, A., and C. Roy. 2013. Autophagy and bacterial infection: an evolving arms race. *Trends in microbiology* 21 (9): 451–456. <https://doi.org/10.1016/j.tim.2013.06.009>.
- Cuesta-Geijo, M., I. García-Dorival, A. Del Puerto, J. Urquiza, I. Galindo, L. Barrado-Gil, F. Lasala, A. Cayuela, C. Sorzano, C. Gil, R. Delgado, and C. Alonso. 2022. New insights into the role of endosomal proteins for African swine fever virus infection. *PLoS pathogens* 18 (1): e1009784. <https://doi.org/10.1371/journal.ppat.1009784>.
- Dixon, L., M. Islam, R. Nash, and A. Reis. 2019a. African swine fever virus evasion of host defences. *Virus research* 266: 25–33. <https://doi.org/10.1016/j.virusres.2019.04.002>.
- Dixon, L., K. Stahl, F. Jori, L. Vial, and D.J.A.R.O.A.B. Pfeiffer. 2020. African Swine Fever Epidemiology and Control. *Annual Review of Animal Biosciences* 8: 221–246. <https://doi.org/10.1146/annurev-animal-021419-083741>.
- Dixon, L., H. Sun, and H.J.A.R. Roberts. 2019b. African swine fever. *Antiviral Research* 165: 34–41. <https://doi.org/10.1016/j.antiviral.2019.02.018>.
- Fensterl, V., J. Wetzel, and G. Sen. 2014. Interferon-induced protein Ifit2 protects mice from infection of the peripheral nervous system by vesicular stomatitis virus. *Journal of virology* 88 (18): 10303–10311. <https://doi.org/10.1128/jvi.01341-14>.
- Forth, J., L. Forth, S. Lycett, L. Bell-Sakyi, G. Keil, S. Blome, S. Calvignac-Spencer, A. Wissgott, J. Krause, D. Höper, H. Kampen, and M. Beer. 2020. Identification of African swine fever virus-like elements in the soft tick genome provides insights into the virus' evolution. *BMC biology* 18 (1): 136. <https://doi.org/10.1186/s12915-020-00865-6>.
- Gao, P., X. Ma, M. Yuan, Y. Yi, G. Liu, M. Wen, W. Jiang, R. Ji, L. Zhu, Z. Tang, Q. Yu, J. Xu, R. Yang, S. Xia, M. Yang, J. Pan, H. Yuan, and H. An. 2021. E3 ligase Nedd4l promotes antiviral innate immunity by catalyzing K29-linked cysteine ubiquitination of TRAF3. *Nature communications* 12 (1): 1194. <https://doi.org/10.1038/s41467-021-21456-1>.
- García-Belmonte, R., D. Pérez-Núñez, M. Pittau, J. Richt, and Y. Revilla. 2019. African Swine Fever Virus Armenia/07 Virulent Strain Controls Interferon Beta Production through the cGAS-STING Pathway. *Journal of virology* 93 (12): e02298-e02218. <https://doi.org/10.1128/jvi.02298-18>.
- Hernaez, B., M. Cabezas, R. Muñoz-Moreno, I. Galindo, M. Cuesta-Geijo, and C. Alonso. 2013. A179L, a new viral Bcl2 homolog targeting Beclin 1 autophagy related protein. *Current molecular medicine* 13 (2): 305–316. <https://doi.org/10.2174/156652413804810736>.
- Huang, L., W. Xu, H. Liu, M. Xue, X. Liu, K. Zhang, L. Hu, J. Li, X. Liu, Z. Xiang, J. Zheng, C. Li, W. Chen, Z. Bu, T. Xiong, and C. Weng. 2021. African Swine Fever Virus p1215L Negatively Regulates cGAS-STING Signaling Pathway through Recruiting RNF138 to Inhibit K63-Linked Ubiquitination of TBK1. *Journal of immunology (Baltimore, Md. : 1950)* 207 (11): 2754–2769. <https://doi.org/10.4049/jimmunol.2100320>.
- Ivashkiv, L., and L. Donlin. 2014. Regulation of type I interferon responses. *Nature reviews. Immunology* 14 (1): 36–49. <https://doi.org/10.1038/nri3581>.

- Li, D., W. Yang, L. Li, P. Li, Z. Ma, J. Zhang, X. Qi, J. Ren, Y. Ru, Q. Niu, Z. Liu, X. Liu, and H. Zheng. 2021a. African Swine Fever Virus MGF-505-7R Negatively Regulates cGAS-STING-Mediated Signaling Pathway. *Journal of immunology (Baltimore, Md. : 1950)* 206 (8): 1844–1857. <https://doi.org/10.4049/jimmunol.2001110>.
- Li, D., J. Zhang, W. Yang, P. Li, Y. Ru, W. Kang, L. Li, Y. Ran, and H. Zheng. 2021b. African swine fever virus protein MGF-505-7R promotes virulence and pathogenesis by inhibiting JAK1- and JAK2-mediated signaling. *The Journal of biological chemistry* 297 (5): 101190. <https://doi.org/10.1016/j.jbc.2021.101190>.
- Li, J., J. Song, L. Kang, L. Huang, S. Zhou, L. Hu, J. Zheng, C. Li, X. Zhang, X. He, D. Zhao, Z. Bu, and C. Weng. 2021c. pMGF505-7R determines pathogenicity of African swine fever virus infection by inhibiting IL-1 $\beta$  and type I IFN production. *PLoS pathogens* 17 (7): e1009733. <https://doi.org/10.1371/journal.ppat.1009733>.
- Li, S., M. Kuang, L. Chen, Y. Li, S. Liu, H. Du, L. Cao, and F. You. 2021d. The mitochondrial protein ERAL1 suppresses RNA virus infection by facilitating RIG-I-like receptor signaling. *Cell reports* 34 (3): 108631. <https://doi.org/10.1016/j.celrep.2020.108631>.
- Liu, H., Z. Zhu, T. Feng, Z. Ma, Q. Xue, P. Wu, P. Li, S. Li, F. Yang, W. Cao, Z. Xue, H. Chen, X. Liu, and H. Zheng. 2021. African Swine Fever Virus E120R Protein Inhibits Interferon Beta Production by Interacting with IRF3 To Block Its Activation. *Journal of virology* 95 (18): e0082421. <https://doi.org/10.1128/jvi.0082421>.
- Liu, S., Y. Luo, Y. Wang, S. Li, Z. Zhao, Y. Bi, J. Sun, R. Peng, H. Song, D. Zhu, Y. Sun, S. Li, L. Zhang, W. Wang, Y. Sun, J. Qi, J. Yan, Y. Shi, X. Zhang, P. Wang, H. Qiu, and G. Gao. 2019. Cryo-EM Structure of the African Swine Fever Virus. *Cell host & microbe* 26 (6): 836–843.e833. <https://doi.org/10.1016/j.chom.2019.11.004>.
- Ma, Z., G. Ni, and B. Damania. 2018. Innate Sensing of DNA Virus Genomes. *Annual review of virology* 5 (1): 341–362. <https://doi.org/10.1146/annurev-virology-092917-043244>.
- O'donnell, V., L. Holinka, D. Gladue, B. Sanford, P. Krug, X. Lu, J. Arzt, B. Reese, C. Carrillo, G. Risatti, and M. Borca. 2015. African Swine Fever Virus Georgia Isolate Harboring Deletions of MGF360 and MGF505 Genes Is Attenuated in Swine and Confers Protection against Challenge with Virulent Parental Virus. *Journal of virology* 89 (11): 6048–6056. <https://doi.org/10.1128/jvi.00554-15>.
- Portugal, R., L. Goatley, R. Husmann, F. Zuckermann, and L. Dixon. 2020. A porcine macrophage cell line that supports high levels of replication of OURT88/3, an attenuated strain of African swine fever virus. *Emerging microbes & infections* 9 (1): 1245–1253. <https://doi.org/10.1080/22221751.2020.1772675>.
- Shen, Z., C. Chen, Y. Yang, Z. Xie, Q. Ao, L. Lv, S. Zhang, H. Chen, R. Hu, H. Chen, and G. Peng. 2020. A novel function of African Swine Fever Virus pE66L in inhibition of host translation by the PKR/eIF2 $\alpha$  pathway. *Journal of virology*. 95 (5): e01872–e01820. <https://doi.org/10.1128/jvi.01872-20>.
- Shimmon, G., J. Hui, T. Wileman, and C. Netherton. 2021. Autophagy impairment by African swine fever virus. *The Journal of general virology* 102 (8): 001637. <https://doi.org/10.1099/jgv.0.001637>.
- Song, G., B. Liu, Z. Li, H. Wu, P. Wang, K. Zhao, G. Jiang, L. Zhang, and C. Gao. 2016. E3 ubiquitin ligase RNF128 promotes innate antiviral immunity through K63-linked ubiquitination of TBK1. *Nature immunology* 17 (12): 1342–1351. <https://doi.org/10.1038/ni.3588>.
- Sun, D., N. Kong, S. Dong, X. Chen, W. Qin, H. Wang, Y. Jiao, H. Zhai, L. Li, F. Gao, L. Yu, H. Zheng, W. Tong, H. Yu, W. Zhang, G. Tong, and T. Shan. 2021a. 2AB protein of Senecavirus A antagonizes selective autophagy and type I interferon production by degrading LC3 and MARCH8. *Autophagy*: 1–13. <https://doi.org/10.1080/15548627.2021.2015740>.
- Sun, E., L. Huang, X. Zhang, J. Zhang, D. Shen, Z. Zhang, Z. Wang, H. Huo, W. Wang, H. Huangfu, W. Wang, F. Li, R. Liu, J. Sun, Z. Tian, W. Xia, Y. Guan, X. He, Y. Zhu, D. Zhao, and Z. Bu. 2021b. Genotype I African swine fever viruses emerged in domestic pigs in China and caused chronic infection. *Emerging microbes & infections* 10 (1): 2183–2193. <https://doi.org/10.1080/22221751.2021.1999779>.
- Sun, M., S. Yu, H. Ge, T. Wang, Y. Li, P. Zhou, L. Pan, Y. Han, Y. Yang, Y. Sun, S. Li, L. Li, and H. Qiu. 2022. The A137R Protein of African Swine Fever Virus Inhibits Type I Interferon Production via the Autophagy-Mediated Lysosomal Degradation of TBK1. *Journal of virology* 96 (9): e0195721. <https://doi.org/10.1128/jvi.01957-21>.
- Sun, P., S. Zhang, X. Qin, X. Chang, X. Cui, H. Li, S. Zhang, H. Gao, P. Wang, Z. Zhang, J. Luo, and Z. Li. 2018. Foot-and-mouth disease virus capsid protein VP2 activates the cellular EIF2S1-ATF4 pathway and induces autophagy via HSPB1. *Autophagy* 14 (2): 336–346. <https://doi.org/10.1080/15548627.2017.1405187>.
- Wang, X., J. Wu, Y. Wu, H. Chen, S. Zhang, J. Li, T. Xin, H. Jia, S. Hou, Y. Jiang, H. Zhu, and X. Guo. 2018. Inhibition of cGAS-STING-TBK1 signaling pathway by DP96R of ASFV China 2018/1. *Biochemical and biophysical research communications* 506 (3): 437–443. <https://doi.org/10.1016/j.bbrc.2018.10.103>.
- Wang, Y., W. Kang, W. Yang, J. Zhang, D. Li, and H. Zheng. 2021. Structure of African Swine Fever Virus and Associated Molecular Mechanisms Underlying Infection and Immunosuppression: A Review. *Frontiers in immunology* 12: 715582. <https://doi.org/10.3389/fimmu.2021.715582>.
- Wang, Z., C. Sheng, C. Yao, H. Chen, D. Wang, and S. Chen. 2019. The EF-Hand Protein CALML6 Suppresses Antiviral Innate Immunity by Impairing IRF3 Dimerization. *Cell reports* 26 (5): 1273–1285.e1275. <https://doi.org/10.1016/j.celrep.2019.01.030>.
- Webb, L., and A. Fernandez-Sesma. 2022. RNA viruses and the cGAS-STING pathway: reframing our understanding of innate immune sensing. *Current opinion in virology* 53: 101206. <https://doi.org/10.1016/j.coviro.2022.101206>.
- Wetzel, J., V. Fensterl, and G. Sen. 2014. Sendai virus pathogenesis in mice is prevented by Ifit2 and exacerbated by interferon. *Journal of virology* 88 (23): 13593–13601. <https://doi.org/10.1128/jvi.02201-14>.
- Wu, Q., M. Schapira, C. Arrowsmith, and D. Barsyte-Lovejoy. 2021. Protein arginine methylation: from enigmatic functions to therapeutic targeting. *Nature reviews. Drug discovery* 20 (7): 509–530. <https://doi.org/10.1038/s41573-021-00159-8>.
- Yan, S., M. Kumari, H. Xiao, C. Jacobs, S. Kochumon, M. Jedrychowski, E. Chouchani, R. Ahmad, and E. Rosen. 2021. IRF3 reduces adipose thermogenesis via ISG15-mediated reprogramming of glycolysis. *The Journal of clinical investigation* 131 (7): e144888. <https://doi.org/10.1172/jci144888>.
- Yang, J., S. Li, T. Feng, X. Zhang, F. Yang, W. Cao, H. Chen, H. Liu, K. Zhang, Z. Zhu, and H. Zheng. 2021a. African Swine Fever Virus F317L Protein Inhibits NF- $\kappa$ B Activation To Evoke Host Immune Response and Promote Viral Replication. *mSphere* 6 (5): e0065821. <https://doi.org/10.1128/mSphere.00658-21>.
- Yang, K., Q. Huang, R. Wang, Y. Zeng, M. Cheng, Y. Xue, C. Shi, L. Ye, W. Yang, Y. Jiang, J. Wang, H. Huang, X. Cao, G. Yang, and C. Wang. 2021b. African swine fever virus MGF505-11R inhibits type I interferon production by negatively regulating the cGAS-STING-mediated signaling pathway. *Veterinary microbiology* 263: 109265. <https://doi.org/10.1016/j.vetmic.2021.109265>.
- Yang, K., Y. Xue, H. Niu, C. Shi, M. Cheng, J. Wang, B. Zou, J. Wang, T. Niu, M. Bao, W. Yang, D. Zhao, Y. Jiang, G. Yang, Y. Zeng, X. Cao, and C. Wang. 2022a. African swine fever virus MGF360-11L negatively regulates cGAS-STING-mediated inhibition of type I interferon production. *Veterinary research* 53 (1): 7. <https://doi.org/10.1186/s13567-022-01025-0>.
- Yang, Y., Y. Huang, and Z. Zeng. 2022b. Advances in cGAS-STING Signaling Pathway and Diseases. *Frontiers in cell and developmental biology* 10: 800393. <https://doi.org/10.3389/fcell.2022.800393>.
- Yoneda, M., J. Hyun, S. Jakubski, S. Saito, A. Nakajima, E. Schiff, and E. Thomas. 2016. Hepatitis B Virus and DNA Stimulation Trigger a Rapid Innate Immune Response through NF- $\kappa$ B. *Journal of immunology (Baltimore, Md. : 1950)* 197 (2): 630–643. <https://doi.org/10.4049/jimmunol.1502677>.
- Zahid, A., H. Ismail, B. Li, and T. Jin. 2020. Molecular and Structural Basis of DNA Sensors in Antiviral Innate Immunity. *Frontiers in immunology* 11: 613039. <https://doi.org/10.3389/fimmu.2020.613039>.
- Zhang, K., B. Yang, C. Shen, T. Zhang, Y. Hao, D. Zhang, H. Liu, X. Shi, G. Li, J. Yang, D. Li, Z. Zhu, H. Tian, F. Yang, Y. Ru, W. Cao, J. Guo, J. He, H. Zheng, and X. Liu. 2022. MGF360-9L Is a Major Virulence Factor Associated with the African Swine Fever Virus by Antagonizing the JAK/STAT Signaling Pathway. *mBio* 13: e0233021. <https://doi.org/10.1128/mbio.02330-21>.
- Zhang, Q., W. Wang, Q. Zhou, C. Chen, W. Yuan, J. Liu, X. Li, and Z.J.M.C. Sun. 2020a. Roles of circRNAs in the tumour microenvironment. *Molecular Cancer* 19 (1): 14. <https://doi.org/10.1186/s12943-019-1125-9>.
- Zhang, Y., M. Li, L. Li, G. Qian, Y. Wang, Z. Chen, J. Liu, C. Fang, F. Huang, D. Guo, Q. Zou, Y. Chu, and D. Yan. 2020b.  $\beta$ -arrestin 2 as an activator of cGAS-STING signaling and target of viral immune evasion. *Nature communications* 11 (1): 6000. <https://doi.org/10.1038/s41467-020-19849-9>.

## Publisher's Note

Springer Nature remains neutral with regard to jurisdictional claims in published maps and institutional affiliations.